Toward an Understanding of Grain-to-Grain Anisotropy Field Variation in Thin Film Media

Jian-Gang Zhu, *Senior Member, IEEE*, Yingguo Peng, and David E. Laughlin

***Abstract*—Grain-to-grain anisotropy field variation has become one of the main causes of medium noise, especially in perpendicular thin film media. In this paper, we present an electron microscopy investigation and theoretical analysis on the grain-to-grain anisotropy field variation in various types of thin film recording media. In alloyed film media, the intrinsic grain-to-grain composition variation would present a lower limit on grain size, thereby limiting area recording density. It is also argued that partial ordering in $L1_0$ materials such as FePt would yield large anisotropy field variation, especially for low values of order parameter.**

***Index Terms*—Anisotropy field, grain, medium noise, order parameter, thin film media.**

I. INTRODUCTION

TRANSITION noise in thin film recording media has been the main factor limiting the area recording density and a driving mechanism for the need of grain size reduction. In longitudinal media, the randomly oriented crystalline anisotropy easy axes of the grains translate into an equivalent 8%–10% ($\Delta H_S/H_S$) standard deviation of the switching field, a significant cause of transition noise at high area recording densities [1]. In perpendicular recording, because of the well oriented crystalline easy axes of the grains along with significant longitudinal field component at a recorded transition, the anisotropy field magnitude variation from grain to grain becomes the dominant factor for medium transition noise, rather than the easy axes orientation distribution. The anisotropy field variation will not only cause transition noise, including both position jitter and amplitude fluctuation, but also broaden the transition length.

Thin film recording media used in hard disk drive applications have been mainly Co-alloys with the *hcp* crystalline structure [2], [3]. For CoCrPt thin film media, one of the most commonly used, increasing Pt concentration (up to 25%) yields a definite increase of anisotropy field by both increasing the uniaxial anisotropy energy constant K_U and reducing the saturation magnetization [4]–[6]. However, increasing the Cr concentration yields the reduction of both the anisotropy energy constant and the saturation magnetization. Thus, any composition variation from grain to grain will yield a corresponding variation of the anisotropy field.

$L1_0$ materials, such as FePt and CoPt, have been proposed as the next generation recording media because of their extremely high-anisotropy field, ~11.5 T at fully ordered phase [7], [8]. However, no practical transducer can produce such a high field. To be utilized in recording applications, the $L1_0$ films or self-assembled nanoparticles must be partially ordered. In this paper, we also explore the role that composition and order parameter variations in $L1_0$ film media.

II. CO-BASED ALLOY THIN FILM MEDIA

A. *CoCrPt*-SiO_x *Perpendicular Thin Film Media*

A transmission electron microscopy (TEM) micrograph of a CoCrPt-SiO_x film sputtered at room temperature is shown in Fig. 1 along with its corresponding cross section TEM micrograph. In this film, grains are all *hcp* with their c axis highly oriented in the direction perpendicular to the film. The image shows well defined grain boundaries and relatively uniform grain size. The grain size roughly follows a Gaussian distribution with a mean diameter about 7.5 nm and a standard deviation of 1.7 nm. The thickness of the medium is approximately 20 nm.

Electron energy loss spectroscopy (EELS) analysis was performed on the medium sample. Fig. 2 shows EELS mapping for cobalt and oxygen. Micrographs are also shown for reference for each element mapping. As shown in the figure, cobalt is mainly distributed in the interior of the grains and oxygen is mainly located in the grain boundaries. EELS mapping also show that the chromium concentration is only slightly higher in the grain boundary than that within the grains.

X-ray energy dispersive spectroscopy (EDS) was utilized to measure the local elementary composition. The obtained spectra show that cobalt has higher concentration within the grain than that in the grain boundaries. Oxygen and silicon are virtually absent inside the grain. Similar to what EELS mapping shows, the EDS spectra show that the chromium concentration is only slightly higher in the grain boundaries as in the interior of the grain. The lack of segregation of chromium to grain boundaries is due to the fact that the film was deposited at room temperature without substrate heating.

Compositions within the individual grains were also measured for this medium by placing the electron beam in the center of the selected grain. Fig. 3 shows the measured atomic percentage of cobalt, platinum, and chromium for 55 selected grains of average size. Since both oxygen and silicon are absent in the interior of a grain, it is a good assumption that the interior of a grain only consists of cobalt, platinum and chromium. The uncertainty in the EDS composition measurement is about

Manuscript received June 14, 2004. This work was supported in part by the Data Storage Systems Center, Carnegie Mellon University, Pittsburgh, PA.

J.-G. Zhu and Y. Peng are with the Department of Electrical and Computer Engineering, Data Storage Systems Center, Carnegie Mellon University, Pittsburgh, PA 15213 USA (e-mail: jzhu@ece.cmu.edu).

D. E. Laughlin is with the Department of Materials Science and Engineering, Data Storage Systems Center, Carnegie Mellon University, Pittsburgh, PA 15213 USA.

Digital Object Identifier 10.1109/TMAG.2004.838074

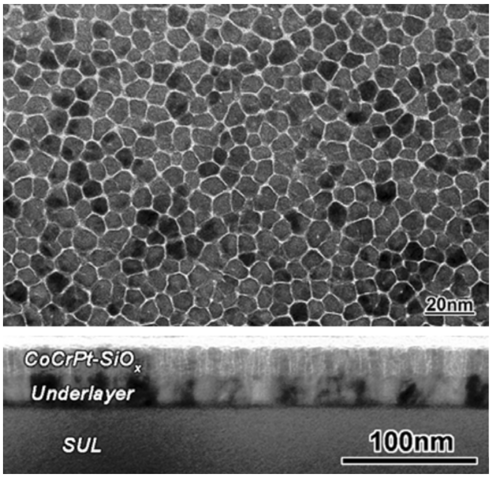

Fig. 1. TEM image of a CoCrPt-SiO$_x$ perpendicular thin film medium, deposited at room temperature.

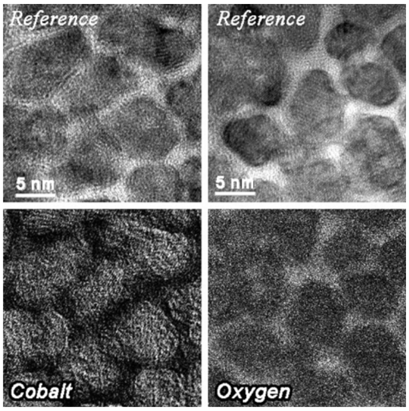

Fig. 2. Element concentration mapping for Co, and O using EELS technique on a CoCrPt-SiO$_x$ granular film. The corresponding TEM micrograph for reference purpose is placed in the top row. Cobalt is mainly distributed within each grain and oxygen is mainly in the grain boundaries.

±0.5%, a scale that is smaller than the size of the symbols used in the plot.

Fig. 4 shows the corresponding histogram for the grain-to-grain composition variation shown in Fig. 4. Note that the measurements only reflect the composition within the grain volume that is illuminated by the electron beam, which is approximately 30 nm^3. The mean composition values for the cobalt, platinum, and chromium are 64%, 23%, and 13%, respectively, and the standard deviations are 1.9%, 1.8%, and 1.6%, respectively.

Since the anisotropy field is a strong function of the element composition, the grain-to-grain composition variation would directly cause the anisotropy field to vary from grain to grain.

B. CoCrPt Longitudinal Thin Film Media

CoCrPt longitudinal thin film medium samples were prepared by sputtering onto substrates that were heated during the deposition process. The film thickness is 10 nm. Individual grain compositions were also studied via the EDS nano-probe method used in the previous case. Fig. 5 shows the histogram of the individual grain compositions over 42 randomly selected average size grains. The grain composition averaged over the 42 grains is 62% cobalt, 27% platinum, and 11% chromium. The standard deviations are 3.3%, 2.9%, and 0.8% for the three elements, respectively. Note that in this case the grain-to-grain variation of chromium concentration is significantly smaller than that in the previous CoCrPt-SiO$_x$ perpendicular medium case, while the variations for cobalt and platinum are greater. It is well known that substrate heating during sputtering in CoCr-alloys yields chromium segregation to grain boundaries [9]–[12]. This mechanism could be responsible for the narrow distribution of Cr concentration among the grains. Since such a feature does not apply to platinum, its grain-to-grain composition variation is larger.

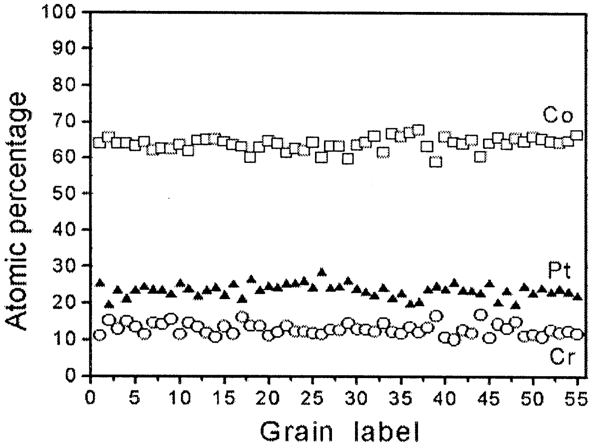

Fig. 3. EDS measurements of composition variations over the interior of 55 randomly selected grains in the CoCrPt-SiO$_x$ film sample. The electron beam illuminating volume is approximately $V = 30$ nm^3 with an effective beam diameter of 1.2 nm. The uncertainty in the measurement is less than 0.5%, smaller than the size of the symbols used in the plot.

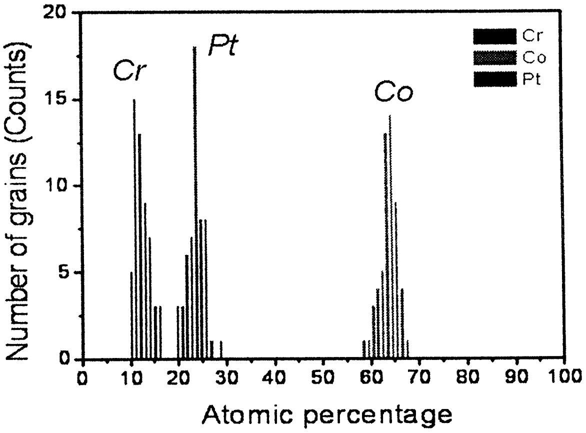

Fig. 4. Histogram of the three elements corresponding to the data shown in Fig. 3.

C. Analysis and Discussion

Alloyed thin film recording media in disk drive applications, either longitudinal or perpendicular, are all cobalt based and consist of platinum for enhancing the magnetocrystalline anisotropy field of the grains. The relative standard deviation of the platinum concentration should be inversely proportional to the square root of the grain volume, assuming a random atomic distribution within a grain. Using the grain-to-grain composition variation data on CoCrPt–SiO$_x$ perpendicular

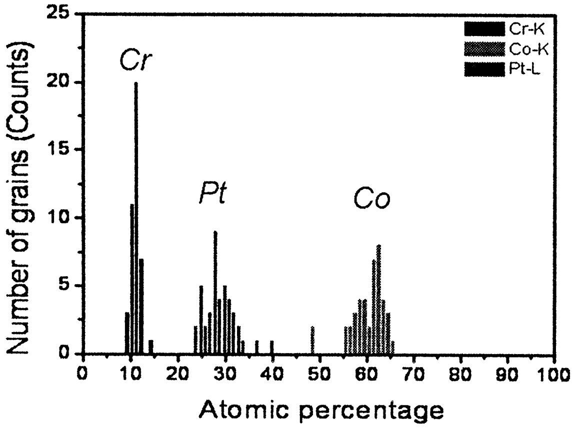

Fig. 5. Histogram of grain compositions in a CoCrPt longitudinal thin film medium sample prepared by sputtering at an elevated substrate temperature.

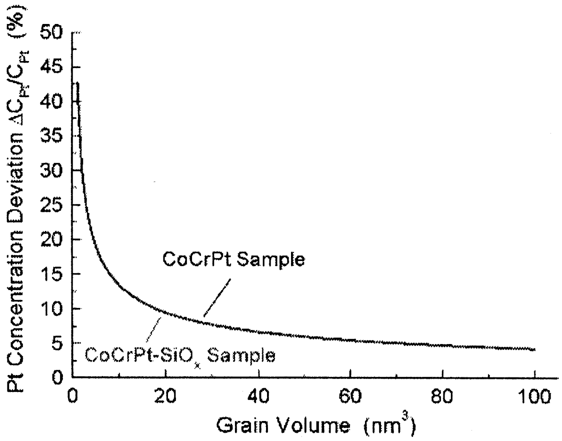

Fig. 6. Predicted relative standard deviation of grain-to-grain platinum concentration variation as a function of grain volume. The nano probe EDS data for the CoCrPt–SiO$_x$ film sample and the CoCrPt film sample are used for calculating the two curves.

film sample and the CoCrPt longitudinal film sample discussed in the previous section, the relative standard deviation as a function of grain volume for the two film samples are

$$\frac{\Delta C_{Pt}}{C_{Pt}} = d\frac{42.7\% \cdot \mathrm{nm}^{3/2}}{\sqrt{V_{\mathrm{grain}}\,(\mathrm{nm}^3)}} \tag{1}$$

for the CoCrPt–SiO$_x$ film sample and

$$\frac{\Delta C_{Pt}}{C_{Pt}} = \frac{42.6\% \cdot \mathrm{nm}^{3/2}}{\sqrt{V_{\mathrm{grain}}\,(\mathrm{nm}^3)}} \tag{2}$$

for the CoCrPt film sample. Equations (1) and (2) are virtually identical. In this analysis, an estimated electron beam illuminating volume vof $V_e = 30\ \mathrm{nm}^3$ is used for the CoCrPt–SiO$_x$ perpendicular medium sample and $V_e = 15\ \mathrm{nm}^3$ is used for the CoCrPt longitudinal medium sample. Both cases are plotted in Fig. 6. Increasing magnetocrystalline anisotropy energy constant will allow for smaller size grains while maintaining their thermal stability. However, reducing grain size yields an increase of the grain-to-grain composition variation with a consequent increase of the anisotropy field variation, thereby, increasing transition noise.

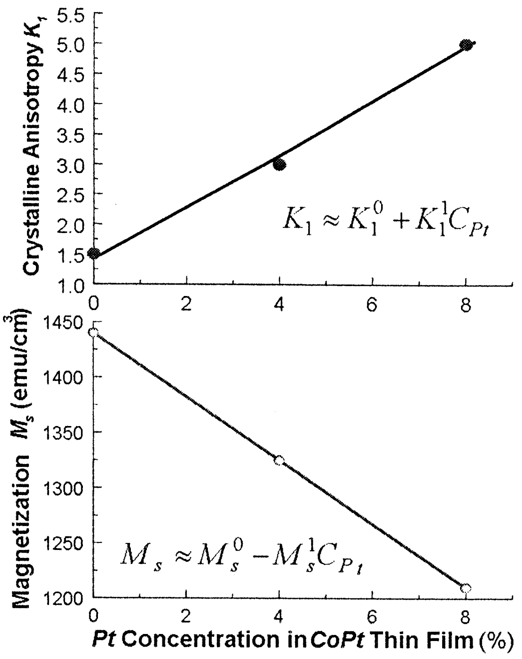

Fig. 7. Experimentally measured crystalline anisotropy energy constant and saturation magnetization as functions of Pt concentration in sputtered uni-crystal CoPt thin film [13].

Fig. 7 shows a set of experimental measurements of the crystalline anisotropy energy constant K_1 and the saturation magnetization M_s as a function of platinum concentration in a longitudinal CoPt thin film [14]. As shown in the figure, increasing the platinum concentration in an *hcp* CoPt alloy yields a significant increase of the anisotropy energy constant and a reduction of the saturation magnetization.

Using the data shown in the figure, one can estimate the anisotropy field variation by assuming the following linear dependences holds:

$$K_1 \approx K_1^0 + K_1^1 C_{Pt} \tag{3}$$

and

$$M_s \approx M_s^0 - M_s^1 C_{Pt} \tag{4}$$

where C_{Pt} is the concentration of platinum in CoPt film.

Thus, the relative variation of the anisotropy field can be written as

$$\frac{\Delta H_k}{H_k} \approx \left(\frac{1}{1+\frac{K_1^0}{K_s^1 C_{Pt}}} + \frac{1}{\frac{M_s^0}{M_s^1 C_{Pt}} - 1}\right) \cdot \frac{\Delta C_{Pt}}{C_{Pt}}. \tag{5}$$

Estimating (3) at $C_{Pt} = 20\%$, one obtains $\Delta H_k/H_k \approx 1.7\Delta C_{Pt}/C_{Pt}$. This demonstrates that the relative standard deviation of the anisotropy field variation and the relative standard deviation of the platinum concentration variation are of the same order of magnitude.

In general, one can always write

$$\frac{\Delta H_k}{H_k} \approx \frac{C_{Pt}}{H_k} \cdot \frac{dH_k}{dC_{Pt}} \cdot \frac{\Delta C_{Pt}}{C_{Pt}}. \tag{6}$$

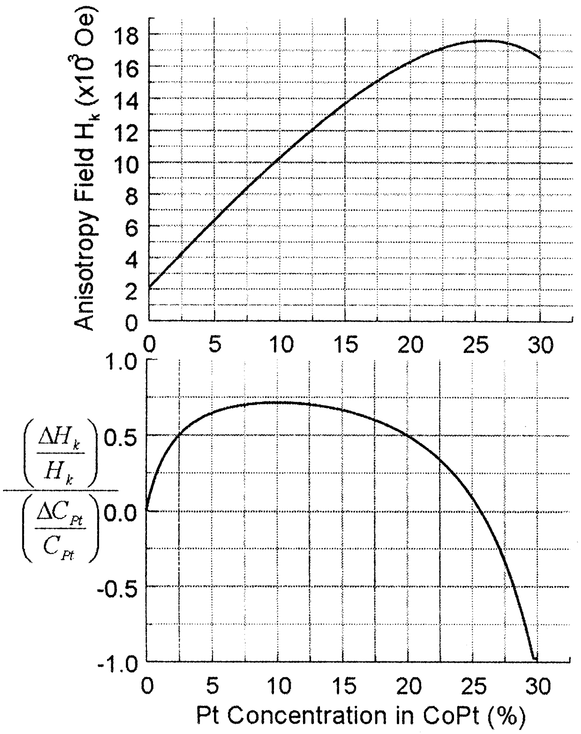

Fig. 8. Fictitious grain anisotropy field dependence as a function of Pt concentration in CoPt thin film and the corresponding ratio between the anisotropy field deviation and composition deviation. Leveling of the anisotropy field at 26% Pt concentration yields zero anisotropy field deviation.

An alloy with a composition that not only yields a high-anisotropy field, but also has a relatively small dependence of the anisotropy field on composition would be ideal. Assuming the anisotropy energy constant and the saturation magnetization have the following dependence on Pt concentration:

$$K_1 = 7 - 0.017\,(C_{Pt} - 0.18)^2 \times 10^6 \text{ erg/cm}^3 \tag{7}$$

and

$$M_S = 1440\text{–}3000 \times C_{Pt} \text{ emu/cm}^3. \tag{8}$$

As shown in Fig. 8, the resulting anisotropy field reaches a maximum at $C_{Pt} = 26\%$ at which the concentration variation yields no anisotropy field variation. Note (7) and (8) have the same initial dependences as the corresponding ones shown in Fig. 7.

The composition variation from grain to grain could also be limited. The narrow distribution of chromium shown in the CoCrPt film deposited at elevated temperature suggests that there exists a way for limiting the grain-to-grain concentration variation.

It is well known that chromium segregates to grain boundaries when the substrate is heated during deposition. A thermodynamic expression for such segregation is given by the Gibbs Adsorption Equation [14]

$$\Gamma_{Cr} \cong -\frac{C_{Cr}}{RT}\left(\frac{\partial \sigma}{\partial C_{Cr}}\right) \tag{9}$$

where Γ_{Cr} is the excess Cr at the grain boundary, σ is the energy of the boundary, and C_{Cr} is the composition of chromium. If chromium decreases the grain boundary energy of the cobalt alloy phase, σ, it will segregate to the boundary, i.e., $\Gamma_{Cr} > 0$. This equation shows that the amount of segregation to the grain boundary is proportional to the amount of chromium in the grain. Thus, more segregation will occur in grains with more chromium. This mechanism self-limits the actual chromium percentage within the grain and the grain-to-grain composition differences will decrease. However, if an alloying element such as platinum does not segregate to the grain boundaries, i.e., $\Gamma_{Pt} = 0$, the platinum composition in each grain will remain as deposited, hence, the grain-to-grain composition variation discussed previously will apply.

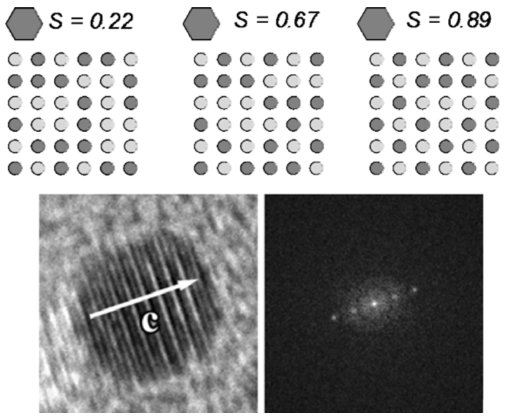

Fig. 9. Illustration of homogeneous ordering with dark and light circles representing Fe and Pt atoms. The bottom TEM image shows a 3 nm partially ordered FePt particle and the corresponding electron diffraction pattern indicating the presence of (110) (Courtesy of M. Tanase).

Therefore, by using elements that segregate, the grain-to-grain composition differences will be smaller. Since the above equation is true only if equilibrium can be reached, sufficient substrate temperature is required for chromium to be able to diffuse. Thus, an optimum temperature may exist for achieving and maximizing the segregation.

III. $L1_0$ RECORDING MEDIA

A. *Homogeneous Ordering*

Homogeneous ordering referred to the mix of ordered and nonordered sites are at the atomic scale. Fig. 9 illustrates the ordering at various values of the order parameter S. The homogeneous ordering can be qualitatively identified via TEM image, as the one of a 3 nm particle shown in the figure. It can also be quantitatively determined by examining the intensity ratio between (110) and (220) in electron diffraction [16].

For homogeneous ordering, theoretical calculation shows that the anisotropy field as a function of the order parameter can be expressed as [15]

$$K_1 = K_1^0 S^2. \tag{10}$$

Since M_S does not vary significantly with the order parameter, one can write

$$H_k = H_k^0 S^2. \tag{11}$$

For a single grain to have an anisotropy field $H_k \approx 1.1$ T, according to the above equation, the order parameter needs to be $S \approx 0.32$.

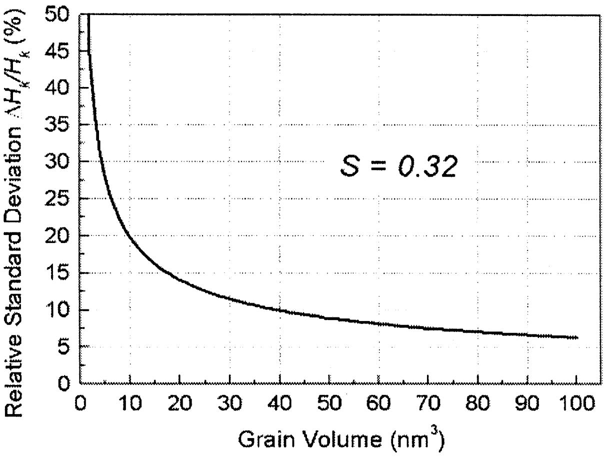

Fig. 10. Calculated relative standard deviation of the grain-to-grain anisotropy field variation for FePt $L1_0$ thin film media.

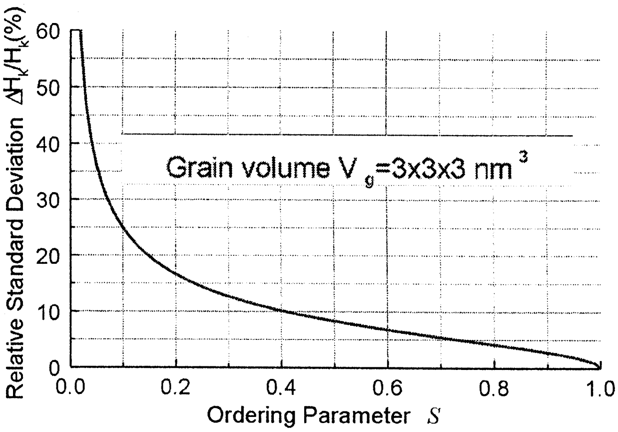

Fig. 11. Relative standard deviation of the anisotropy field variation as a function of ordering parameter for $L1_0$ recording media.

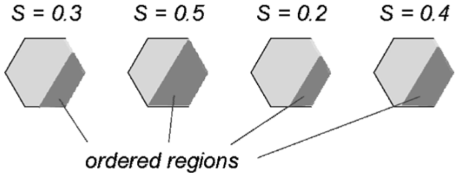

Fig. 12. Illustration of heterogeneous ordering, characterized by separation of a full ordered region and nonordered region.

Now consider an assembly of identical FePt grains, each within a grain has an equal probability S, which is the order parameter, to order, the relative standard deviation of the order parameter from grain to grain is

$$\frac{\Delta S}{S} = \sqrt{\frac{V_c}{V_g}\left(\frac{1}{S} - 1\right)} \tag{12}$$

with a volume V_g. Assuming each unit cell, with volume V_c. Thus, the relative standard deviation of the grain-to-grain anisotropy field variation can be written as

$$\frac{\Delta H_k}{H_k} = \frac{2\Delta S}{S} = \sqrt{\frac{4V_c}{V_g}\left(\frac{1}{S} - 1\right)}. \tag{13}$$

Fig. 10 plots the above equation as a function of grain volume for $S = 0.32$. For a grain with a volume around 100 nm^3, the relative deviation of the anisotropy field is about 7%. For a 30 nm^3 grain, the deviation is around 11%. Fig. 11 plots the relative deviation as a function of the order parameter S for a grain volume of $3 \times 3 \times 3$ (nm^3). The deviation becomes significant at low values of the order parameter.

B. Heterogeneous Ordering

If full ordering occurs only in parts of a grain while leaving the rest of the grain completely nonordered, it is referred to as heterogeneous ordering, illustrated in Fig. 12. The order parameter of a grain in this case is simply the volumetric percentage of the ordered region. Heterogeneous ordering has been observed in sputtered FePt $L1_0$ films by TEM study [17] and it is expected to yield much more severe grain-to-grain variation of the order parameter as compared to the homogeneous ordering case when a full ordering is not achieved.

Heterogeneous ordering is likely to occur in the schemes that use a small amount additive element to assist ordering process. For example, a method that uses either Au or Ag as additional element to FePt alloy has been proposed for reducing the ordering temperature [18], [19]. Since local ordering is likely to depend on the concentration of the additive element as well as its spatial distribution within a grain, significant grain-to-grain order parameter variation could occur when the system is partially ordered.

The spatial separation of the ordered and nonordered region within a grain will result in relatively complex micromagnetic processes during a magnetization reversal, causing the reversal field threshold to be a strong function of not only the order parameter, but also the location of the ordered region and the size of the grain. The resulted grain-to-grain effective anisotropy field variation could be so severe that the medium becomes nonsuitable for high-density recording applications.

Heterogeneous ordering also opens up the possibility for variants within a grain, which would yield severe reduction of the effective anisotropy field.

IV. CONCLUSION AND REMARKS

In *hcp* CoPt-based alloy film media, the statistical variation of the platinum concentration from grain to grain can cause a corresponding anisotropy field variation if the anisotropy field strongly depends on Pt concentration. Since the relative variance of the platinum concentration is inversely proportional to grain volume, a minimum allowable anisotropy field variation in ultrahigh-density recording will set a lower limit on the grain volume. We also pointed out that if one can find a substitute for platinum that not only sufficiently enhances the anisotropy field, but also segregates to grain boundaries, it may be possible to produce film media with a well defined concentration inside every grain.

Grain-to-grain anisotropy field variation for partially ordered $L1_0$-FePt media has been analyzed. An analytical formulation of the anisotropy field variation has been obtained as a function of both order parameter and grain volume for homogeneous ordering. For the grain volume required at recording densities approaching 1 $\mathrm{Tbits/in}^2$, the predicted anisotropy field variation would be considered very significant if the order parameter is below 0.7. For heterogeneous ordering, the resulted grain-to-grain effective anisotropy field variation is expected to be far more severe, mainly due to the resulted magnetically "soft" phase within a grain. This argument can be extended to systems that use either Pd to substitute Pt or Ni to substitute Fe for achieving adequate anisotropy field for recording applications. In such systems, it has been shown that separation of magnetically "hard" and "soft" phases occurs within a grain [20]. Such phase segregation is likely to make the effective anisotropy field strongly depend on the spatial distribution of the two phases as well as the grain size, thereby, causing large grain-to-grain anisotropy field variation.

ACKNOWLEDGMENT

The authors would like to thank Dr. G. Bertero and the Komag Corporation for providing the CoCrPt-SiO_x perpendicular medium.

REFERENCES

[1] J. Zhu, unpublished results.
[2] B. Lu and D. E. Laughlin, "Microstructure of longitudinal media," in *The Physics of Ultrahigh-Density Magnetic Recording*. ser. Springer Series in Surface Sciences, M. Plumer, J. Van Ek, D. Weller, and G. Ertl, Eds. New York: Springer-Verlag, 2001, vol. 41.
[3] T. C. Arnoldussen, "Film media," in *Magnetic Recording Technology*, C. D. Mee and E. D. Daniel, Eds. Piscataway, NJ: IEEE Press, 1995, ch. 4, pp. 4.1–4.59.
[4] T. Yogi, T. A. Nguyen, S. E. Lambert, G. L. Gorman, and G. Castillo, "Role of atomic mobility in the transition noise of longitudinal media," *IEEE Trans. Magn.*, vol. 26, no. 5, pp. 1578–1580, Sep. 1990.
[5] I. L. Sanders, T. Yogi, J. K. Howard, S. E. Lambert, G. L. Gorman, and C. Hwang, "Dependence of magnetics, microstructures and recording properties on underlayer thickness in CoNiCr/Cr media," *IEEE Trans. Magn.*, vol. 25, no. 5, pp. 3869–3869, Sep. 1989.
[6] T. Shimizu, Y. Ikeda, and S. Takayama, "CoPtCr composite magnetic thin films," *IEEE Trans. Magn.*, vol. 28, no. 5, pp. 3102–3104, Sep. 1992.
[7] S. Sun, C. B. Murray, D. Weller, L. Folks, and A. Moser, "Monodisperse FePt nanoparticles and ferromagnetic FePt nanocrystal superlattices," *Science*, vol. 287, pp. 1989–1991, 2000.
[8] S. Jeong, Y.-N. Hsu, D. E. Laughlin, and M. E. McHenry, "Magnetic properties of nanostructured CoPt and FePt thin films," *IEEE Trans. Magn.*, vol. 36, no. 5, pp. 2336–2338, Sep. 2000.
[9] M. Futamoto, N. Inaba, Y. Hirayama, K. Ito, and Y. Honda, "Compositional microstructure and micromagnetics of Co-based thin film recording media," in *Proc. Mat. Res. Soc. Symp.*, vol. 517, 1998, pp. 243–254.
[10] M. R. Kim, S. Guruswamy, and K. E. Johnson, "Experimental observation of solute segregation in longitudinal CoPtCr/cr magnetic thin films," *IEEE Trans. Magn.*, vol. 29, no. 6, pp. 3673–3675, Nov. 1993.
[11] N. Inaba, T. Yamamoto, Y. Hosoe, and M. Futamoto, "Microstructural segregation in CoCrTa and CoCrPt longitudinal magnetic recording media," *J. Magn. Magn. Mater.*, vol. 168, pp. 222–231, 1997.
[12] J. E. Wittig, T. P. Nolan, C. A. Ross, M. E. Schabes, K. Tang, R. Sinclair, and J. Bentley, "Chromium segregation in CoCrTa/Cr and CoCrPt/Cr thin films for longitudinal recording media," *IEEE Trans. Magn.*, vol. 34, no. 4, pp. 1564–1567, Jul. 1998.
[13] W. Yang, "Determining co-alloy anisotropy constants via epitaxial unicrystal film," Ph.D. dissertation, Dept. Electr. Comput. Eng., Carnegie Mellon Univ., Pittsburgh, PA, 2000.
[14] R. T. DeHoff, *Thermodynamics in Materials Science*. New York: McGraw-Hill, Inc., 1993.
[15] S. Jeong, "Structure and magnetic properties of polycrystalline fept and copt thin films for high density recording media," Ph.D. dissertation, Carnegie Mellon Univ., Pittsburgh, PA, 2002.
[16] K. Sato and Y. Hirotsu, "Long-range order parameter of oriented $L1_0$-FePt nanoparticles determined by elecron diffraction," *Mater. Translations*, vol. 44, no. 8, pp. 1518–1522, 2003.
[17] R. A. Ristau, K. Barmak, L. H. Lewis, K. R. Coffey, and J. K. Howard, "On the relationship of high coercivity and $L1_0$ ordered phase in CoPt and FePt thin films," *J.Appl. Phys.*, vol. 86, pp. 4527–4533, 1999.
[18] S. Wang, S. S. Kang, D. E. Nikles, J. W. Harrell, and X. W. Wu, "Magnetic properties of self-organized $L1_0$ FePtAg nanoparticle arrays," *J. Magn. Magn. Mater.*, vol. 266, pp. 49–56, 2003.
[19] S. Kang, Z. Jia, D. E. Nikles, and J. W. Harrell, "Synthesis, self-assembly, and magnetic properties of $[\mathrm{FePt}]_{1-x}\mathrm{Au}_x$ nanoparticles," *IEEE Trans. Magn.*, vol. 39, no. 5, pp. 2753–2757, Sep. 2003.
[20] S. D. Willoughby, J. M. MacLaren, T. Ohkubo, S. Jeong, M. McHenry, D. E. Laughlin, S.-J. Choi, and S.-J. Kwon, "Electronic, magnetic, and structural properties of $L1_0$ $\mathrm{FePt}_x\mathrm{Pd}_{1-x}$ alloys," *J. Appl. Phys.*, vol. 91 (10), pp. 8822–8824, May 2002.